Development of an Expedient Two-Stage Gas Gun

Finn van Donkelaar

A thesis
submitted in partial fulfillment of the
requirements for the degree of

Master of Science in Aeronautics and Astronautics

University of Washington

2021

Committee:
Carl Knowlen
Robert Breidenthal

Program Authorized to Offer Degree:
Aeronautics and Astronautics

University of Washington

Abstract

Development of an Expedient Two-Stage Gas Gun

Finn van Donkelaar

Chair of the Supervisory Committee:
Dr. Carl Knowlen
Aeronautics and Astronautics

The ram accelerator is a hypervelocity launcher that accelerates projectiles through a tube filled with gaseous propellant. Combustion is initiated by the passage of the projectile and will overtake the projectile unless it enters the tube at a sufficiently high Mach number. With economical propellant mixtures such as methane/air, the projectile must be launched into the tube at approximately 1000 m/s. This limit on ram operation restricts projectile launch duties in smoothbore ram accelerators to powder guns and light gas guns.

The baffled-tube ram accelerator (BTRA) retards the travel of the combustion-driven shock front with a series of baffles, preventing combustion from overtaking the projectile at low Mach numbers. Recent experiments with low velocity starting in the University of Washington's BTRA have confirmed that successful ram operation can occur at a projectile entrance velocity of 650 m/s in a BTRA operating with methane/air propellant. These results open the door to using poorer-performing launchers than have previously been contemplated for ram projectile launch.

A subscale two-stage gas gun was constructed to determine the feasibility of ram starting with a gun that achieves these low entrance velocities through pressure and temperature multiplication of an extremely low-cost propellant, such as nitrogen or compressed air. Projectile launch conditions were predicted with the isentropic relations and gun performance was compared to a model of a single-stage infinite-

breech gas gun. A high-speed camera was used to directly measure muzzle velocity and to infer pressure at the nozzle. The measured ballistic efficiency of the launcher indicates that substantial increases in propellant temperature and pressure were achieved, in line with predictions.

Contents

LIST OF FIGURES

NOMENCLATURE

All quantities in MKS unless otherwise specified.

P	Pressure
T	Temperature
γ	Ratio of specific heats
D	Diameter
ρ	Density
a	Sound speed
m	Mass
M	Mach number

LIST OF ABBREVIATIONS

BTRA: Baffled-Tube Ram Accelerator

MoC: Method of Characteristics

UW: University of Washington

TSGG: Two-Stage Gas Gun

LGG: Light Gas Gun

ID: Inner Diameter

OD: Outer Diameter

ICE: Internal Combustion Engine

ACKNOWLEDGEMENTS

Thank you to my advisor, Dr. Carl Knowlen, for the wealth of knowledge that he has provided to me. Not just in the theoretical aspects of gasdynamics and combustion, but also the practical tricks and tips needed to make an experiment really work. I would also like to thank Dr. Robert Breidenthal for being on my thesis committee and for sparking my interest in supersonic jets of all kinds with his course on compressible fluids.

Thank you to the research assistants who provided me with advice and tolerated the absolute mess that I made of the lab (and my house) while manufacturing and testing this experiment. Brian Leege, Chase Smith, Adrian Lo, Kristina Dong, Richard Egbert, Carter Vu, Navid Daneshvaran, and Benjamin Hlavsa.

Chapter 1

INTRODUCTION

The ram accelerator is a hypervelocity launcher with the potential to be used for space launch applications. As in other impulsive launch methods, the goal of ram accelerator space launch is to give a space vehicle sufficient initial velocity to substantially reduce the amount of propellant that it must carry to reach orbit. The propulsive cycle of a ram accelerator is analogous to a ramjet engine.

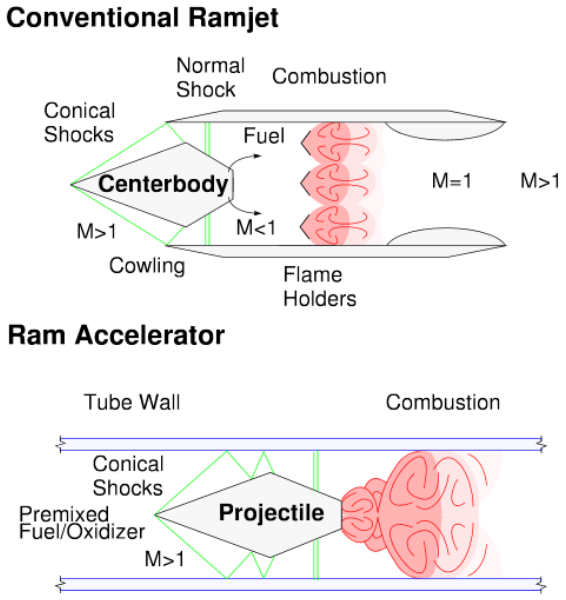

Fig. 1: Propulsive cycle comparison.

In a ramjet engine, a centerbody compresses atmospheric air via a system of conical shocks as the air travels into the cowling which is attached to the centerbody. Fuel is combusted with the compressed air and the combustion gas is exhausted through a converging-diverging nozzle to produce thrust. The ram accelerator replaces the cowling with a tube which engages slidably with the centerbody, now called a

projectile. Instead of intaking atmospheric air, the tube is prefilled with a combustible mixture. As the projectile travels through the tube, it initiates combustion in the mixture and the resulting combustion gas exerts force on the base of the projectile. By using a propellant that is essentially stationary in the lab frame of reference before encountering the projectile and after combustion is complete, the ram accelerator avoids the gasdynamic limitations on muzzle velocity that guns possess [1].

The ramjet and the ram accelerator share the limitation of requiring some minimum Mach number in order to achieve steady operation. If a projectile enters the tube of a ram accelerator at a Mach number below approximately 2.4, combustion will overtake the projectile in a phenomenon known as an "unstart" and the projectile will rapidly decelerate [2]. It is possible to achieve steady ram acceleration at low initial velocities by employing mixtures of gases which have a low sound speed, and which release relatively low amounts of combustion energy. However, for reasons of compactness and cost, it is desirable to use lighter and more energetic gas mixtures. The starting velocities required for most of these mixtures are in the range of 1 km/s.

The baffled-tube ram accelerator (BTRA) is a refinement on the original ram accelerator concept which replaces the smooth wall of the tube with a series of washer-like baffles.

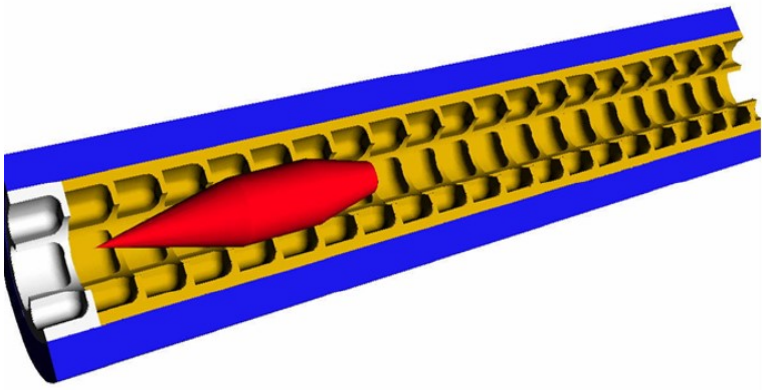

Fig. 2: Baffled-Tube Ram Accelerator.

The inner diameter of these baffles is approximately equal to the diameter of the projectile. The temporary sliding seal formed between the projectile body and the baffles retards the travel of combustion gas from the base of the projectile to the nose of the projectile, preventing unstart over a wide range of operating conditions. Although the BTRA was originally intended to enable the use of extremely energetic gas mixtures, recent experiments have shown its utility in the role of low-speed start. Steady ram operation has been achieved at initial velocities as low as 650 m/s in methane/air mixtures, corresponding to a Mach number of 1.8 [3].

These low velocities enable the use of a wide range of cost-effective projectile launch technologies which previously were considered to have insufficient performance for ram accelerator start duties. The specific technology that this work focuses on is the two-stage gas gun (TSGG) using air or nitrogen as a propellant (Fig. 3).

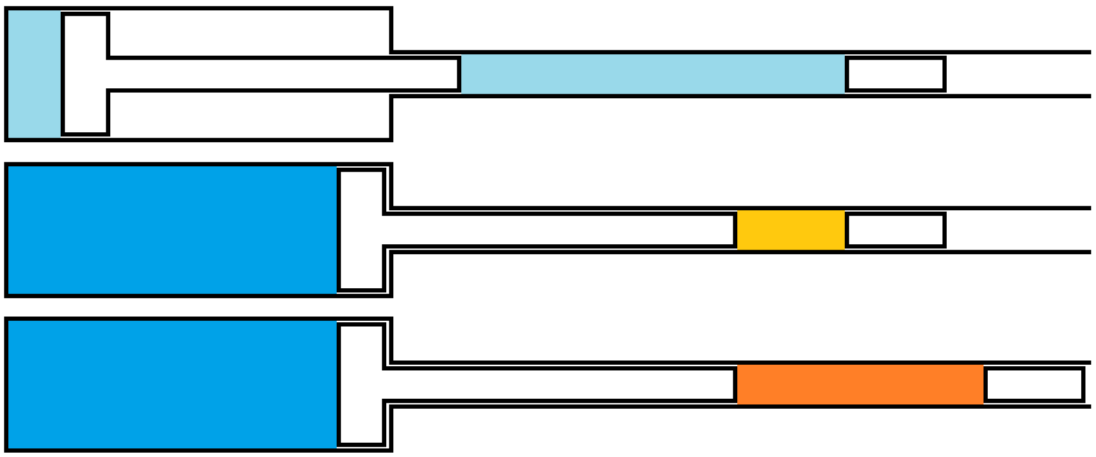

Fig. 3: Two-stage gas gun.

In a TSGG, a reservoir of room-temperature propellant gas behind the projectile (the "driven section") is compressed by the rapid movement of a piston. The piston is driven by the expansion of a gas in a second reservoir (the "driving section"). The compression process is approximately adiabatic, and the temperature of the propellant gas can

increase by a factor of 15 in extreme cases [4]. A substantial increase in temperature is essential for achieving projectile velocities above approximately 400 m/s while using a heavy gas like nitrogen or air as the propellant.

A TSGG with a bore diameter of ½" and a barrel length of 18" was constructed to investigate the feasibility of using this technology for ram starting duty. The goals of this project were 1) to demonstrate muzzle velocities which are unattainable with heavy gases at room temperature, 2) to validate simple models of TSGG operation, 3) to create a subscale model of a TSGG for UW ram accelerator launch duties which would be constructed by modifying the existing laboratory LGG. Projectile velocity was measured with a Phantom v1211 high-speed camera recording at 50,000 frames per second. The velocimetry videorecording was also used to infer the residual pressure at the muzzle of the gun by using an empirical correlation to relate the barrel shock dimensions to the stagnation pressure. The motion of the piston was modeled with a numerical implementation of the isentropic relations for an ideal gas. The acceleration of the projectile was modeled for the case of an infinite breech as a point of comparison. The closure of the UW AA machine shop prior to the start of the project gave the TSGG an improvised character. All but one of the gun components were fabricated using a laboratory drill press and a few hand tools. This aspect of the project motivated the inclusion of "Expedient" in the title of this thesis and will explain the appearance of the experimental setup shown in Chapter 3.

Chapter 2

THEORETICAL MODELS

The piston attained a maximum Mach number of 0.175 during the compression stroke, placing its motion well within the bounds of subsonic flow. A MoC code was unnecessary for this calculation, so the task of modeling the piston motion was considerably simplified. A one-step Forwards Euler numerical code was written in Matlab to calculate the piston motion using the isentropic relations for an ideal gas.

2.1 Piston Motion Code

The compression stroke of the piston occurs over a period of approximately 5 milliseconds, resulting in minimal heat transfer from the propellant gas to the tube walls. The isentropic relations can then be used to predict the motion of the piston and the properties of the propellant gas at the time of firing.

$$T_2 = T_1 * \left(\frac{V_2}{V_1}\right)^{\gamma-1} \tag{2.1}$$

$$P_2 = P_1 * \left(\frac{V_2}{V_1}\right)^{\gamma} \tag{2.2}$$

Typical output for the code is shown below. An important feature of rapid, single-stroke compression to a high volumetric compression ratio is the extremely rapid change in gas temperature and pressure which occurs near the end of the compression stroke. Small changes in the driving or driven section initial pressures are magnified by the compression process and will produce highly variable conditions at the end of the compression stroke.

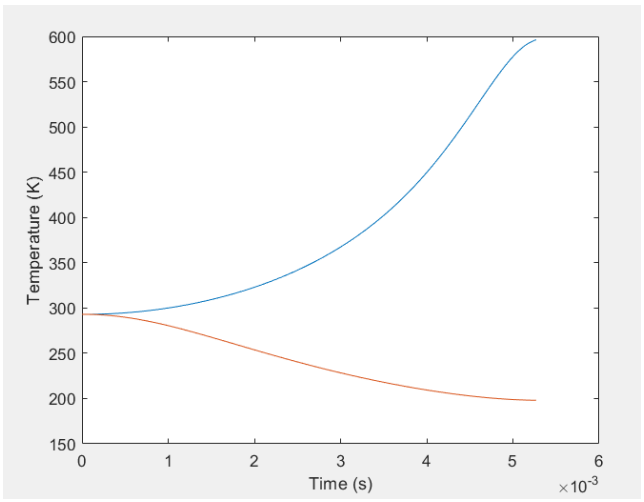

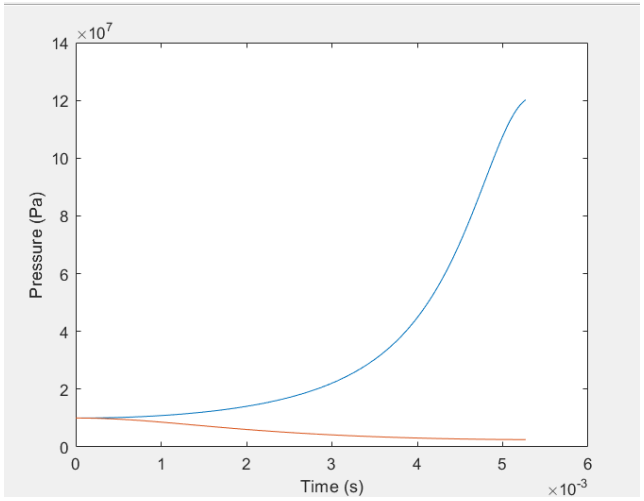

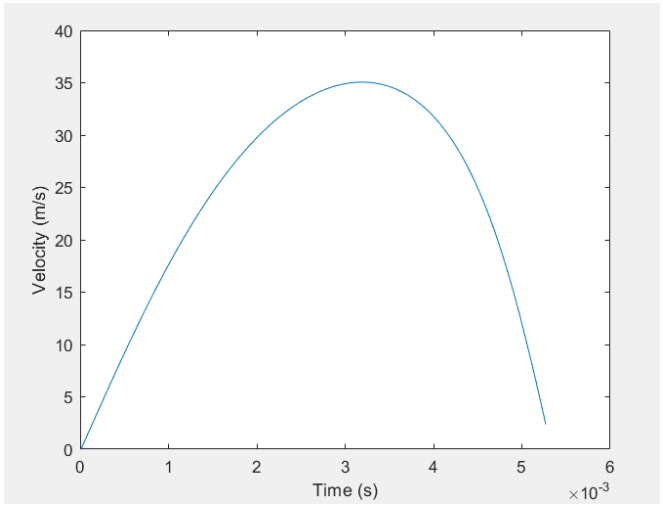

Fig. 4: Temperature, pressure, and piston velocity outputs.

The rapid change in gas conditions and piston velocity can be seen more clearly when the relevant variables are plotted together (Fig. 5). Within a period of about one millisecond, the temperature increases by 30%, the pressure triples and the piston stagnates.

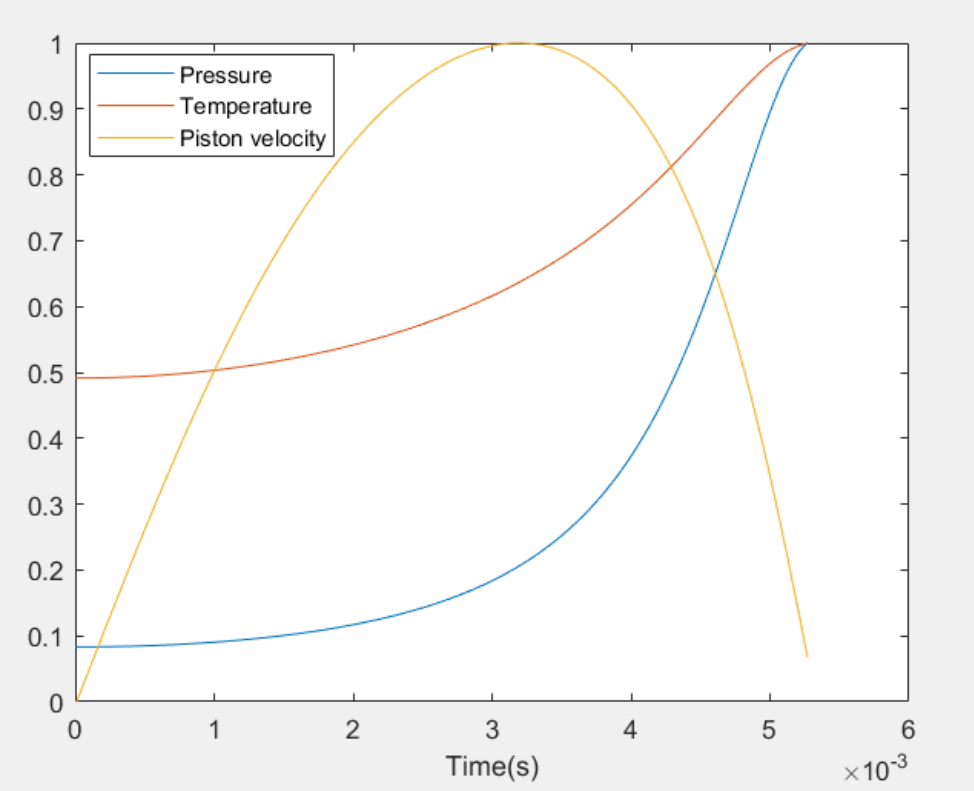

Fig. 5: Normalized outputs plotted together.

It is clear that the much of the theoretical performance of the TSGG is gained within this time. However, the improvised nature of the experimental setup demanded less extreme projectile launch conditions. The accuracy of the gas supply regulator and of the machining methods used to construct the gun were not sufficient to guarantee repeatable shots at high pressure. In practice, the gun was limited to a firing pressure of 10,500 psi (72 MPa) instead of the approximately 17,000 psi (120 MPa) that it was theoretically capable of. This effort to reduce variability in launch conditions is also what motivated the fill process described in Chapter 3.

2.2 Projectile Motion Code

As a means of comparison, a Matlab code was written which implemented Seigel's [5] equation for the unsteady expansion of a gas behind a projectile for the case of an infinite-breech gun. This code served to quantify the practical benefit of dividing the nitrogen supply into a driving and driven section instead of simply propelling the projectile with a single large volume of gas which did not possess augmented pressure or temperature. The overall gain in velocity was 20%-25%.

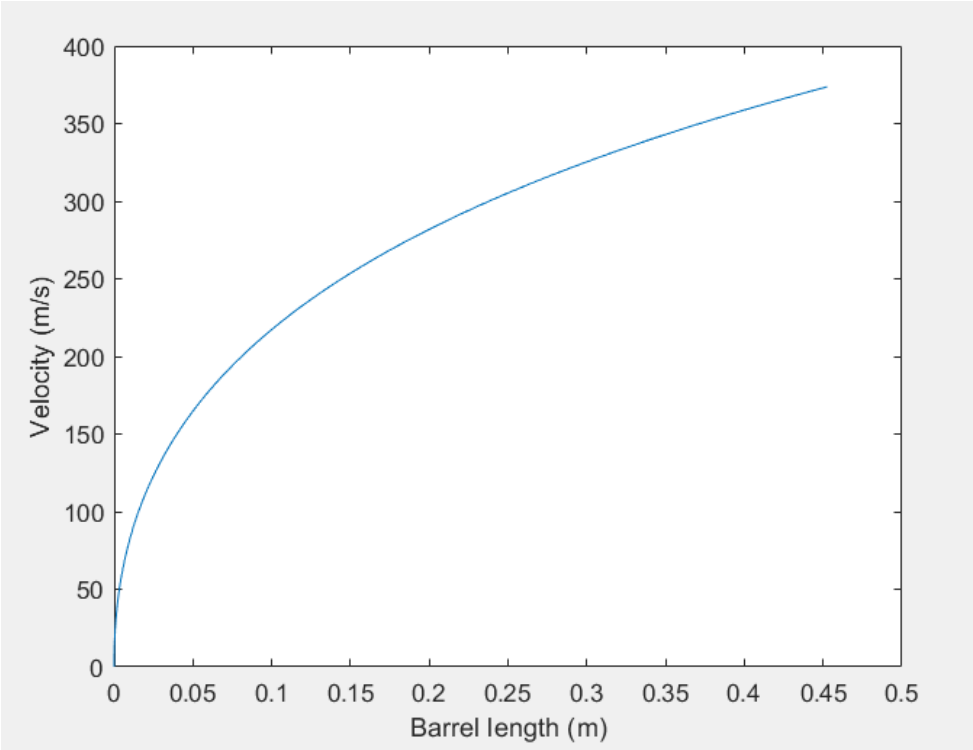

Fig. 6: Increase in velocity with barrel length for a 3.25 g projectile propelled by 1400 psi nitrogen at room temperature.

Chapter 3

EXPERIMENTAL APPARATUS AND METHODOLOGY

The TSGG constructed for this project was a series of tubes fitted concentrically together. The ID of the tube used to construct the driving section was 1.25," producing a driving/driven area ratio of 6.25. The importance of the area ratio to gun performance was described in Chapter 2. This relatively low area ratio was chosen for similarity to a potential future TSGG which would use the existing laboratory LGG body, not to maximize performance.

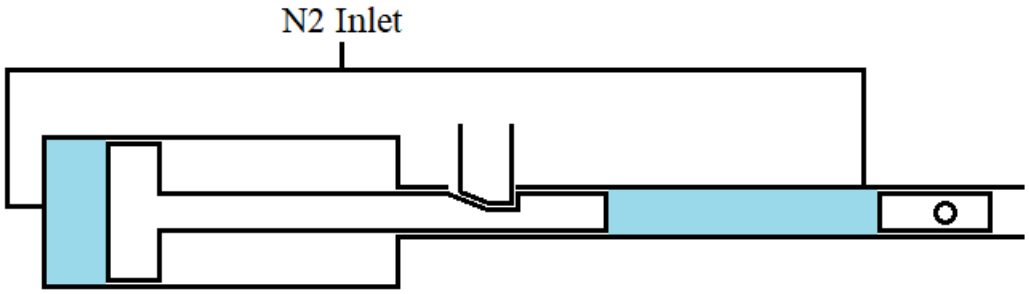

Fig. 7: TSGG schematic.

3.1 Gun Construction

The basic construction of the TSGG is shown in Fig. 7. Regulated nitrogen flows to the driven section and to the driving section. The piston is retained by a lever which penetrates through a slot in the driven section tube and engages with a notch in the piston shaft. The projectile is retained until the compression stroke is complete by an aluminum shear pin which transfixes the projectile and the barrel.

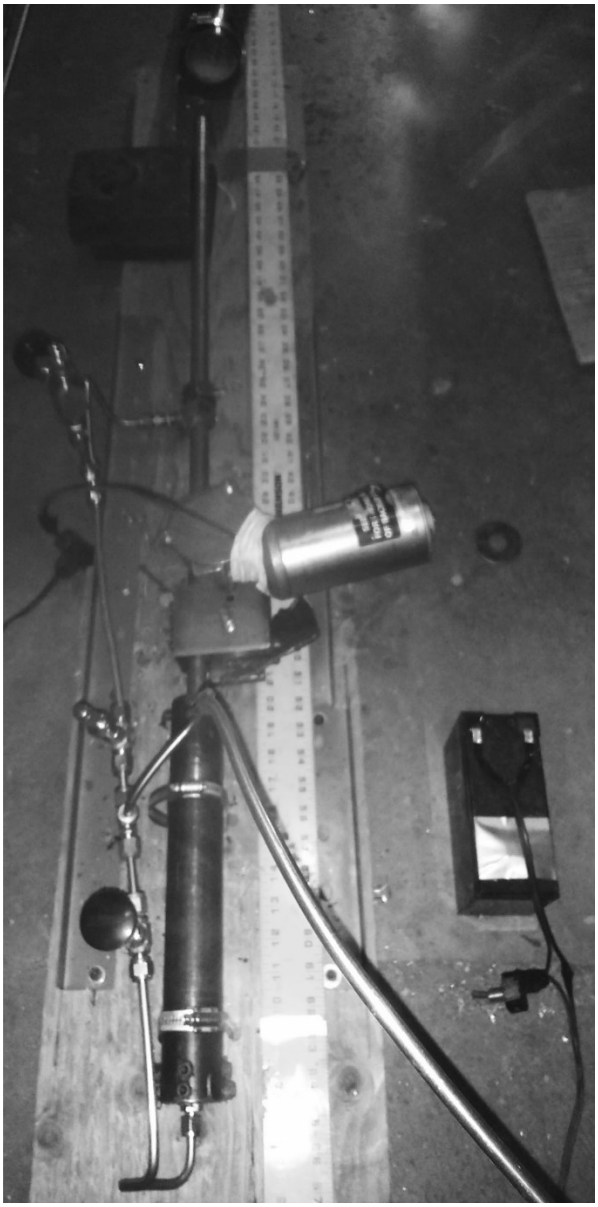

Fig. 8: Gun assembly pictured from the rear of the driving section.

3.1.1 Piston

The piston was constructed from a 14″ length of ½″-13 steel threaded rod and had a total mass of 350 grams. The driven end of the piston had an aluminum extension with an attached o-ring. The o-ring groove was constructed in the same fashion as the projectile grooves (Section 3.1.2).

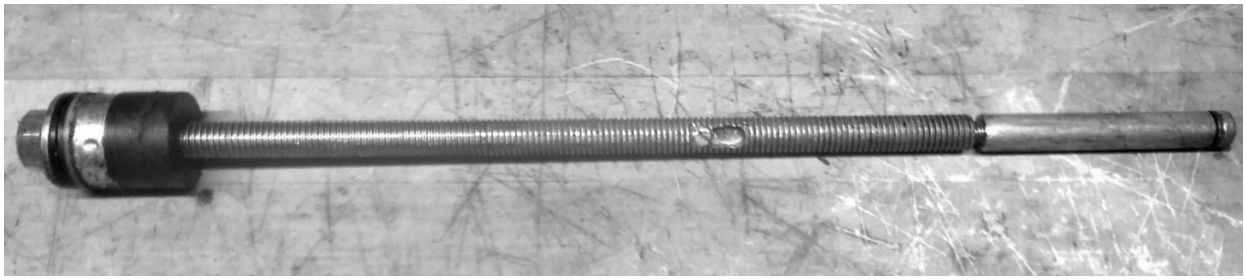

Fig. 9: Left to right: Clamping nut, seal washers, seal support, buffer pad, retaining notch and set screw, piston extension, piston head o-ring.

The driving end of the piston was capped with a ½"-13 nut which was used to clamp the rubber washers which sealed the driving section. The rubber washers were located between two aluminum washers which transferred force from the clamping nut. After the washers, a 3/8" thick aluminum donut served to provide structural support to the seals. The donut was tapped to ½"-13 on its interior surface and was threaded on to the piston shaft. A rubber buffer pad with the same threading followed the donut and prevented damage to the driving end when the piston decelerated at the end of the compression stroke.

The retaining notch was milled into the piston shaft with a ¼" cutter on a laboratory drill press. An 8-32 set screw was threaded into the shaft at one end of the notch to serve as a wear surface for the release lever and to adjust the position of the release lever at the time of firing.

3.1.2 Projectiles and Shear Pin

Each projectile was cut from a piece of ½" diameter round stock. Data was collected with both aluminum and polycarbonate projectiles. After cutting to length, an o-ring groove was cut into the projectile body by chucking the projectiles in a laboratory drill press and carefully applying a hacksaw to the projectile body with the drill press switched on. Final adjustment of the notch and chamfering of the projectile edges was performed with a file. Each projectile was provided with a ½" OD x 1/16" thick o-ring.

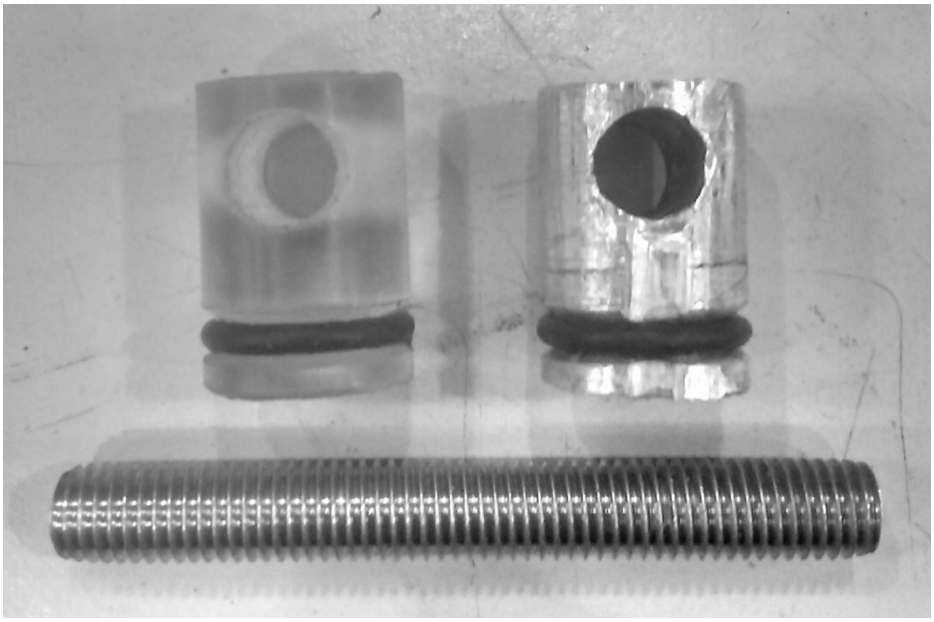

Fig. 10: Polycarbonate (left) projectile, aluminum (right) projectile, and shear pin.

The through-holes in the projectile which engaged the aluminum shear pin were drilled on the drill press using a jig to accurately locate the holes. The shear pin used in every experiment was a 2″ length of ¼″-28 6061 aluminum threaded rod with a shear strength of 30,000 psi. Due to the extremely short timescale over which the pressure in the driven section increased, it was necessary to check the strain rate sensitivity of 6061-T6 aluminum so that strain rate effects on stress could be quantified. The high strain rate was found to increase the stress on the pin by 1,450 psi [6], which was accounted for in the breaking pressure calculations (Chapter 4).

The shear pin fixture was constructed from a ¾″ nut which was drilled out to ¾″ ID and fitted over the barrel. A centered hole was drilled through the nut and tapped to 1/4″-28 to receive the shear pin. It was necessary to use a threaded shear pin and fitting because the forward travel of the projectile would expose the fitting to the pressurized driven section. An unthreaded shear pin would have been blown out of the fitting holes.

Fig. 11: Shear pin fixture (top) and driven section gas supply line (bottom).

The driven section gas supply line was located directly behind the projectile so that the piston head would not have to travel past the supply line hole during the compression stroke. The sharp edges of the hole would have torn the piston head o-ring and the gun would have required disassembly after each shot to maintain the piston head seal.

Locating the supply line next to the projectile created a new problem of backflow into the supply line during the compression stroke. This issue was successfully solved with the addition of an improvised check valve made from a ¼" Allan screw to the inside of the supply line fitting. The check valve was made on the drill press with a hacksaw and file in the same manner that the projectiles were.

3.1.3 Release Lever and Sear

The difference in piston area between the driving section and the driven section produced a net force which was used to increase the pressure and temperature of the driven section. Until the pressurization of each section was complete, this

approximately 6600 N load was carried by the release lever and transferred to the release lever pivot through a ½″-13 threaded rod.

The release lever pivot was constructed out of a 1 ½″ thick block of stainless steel. It carried mounting holes for the release lever pivot and the servomotor. The pivot was affixed to the barrel by four ¼″ bolts. The release lever and sear required a ½″ wide slot to rotate within. Milling this slot was the only machining operation for this project that was not performed on a laboratory drill press.

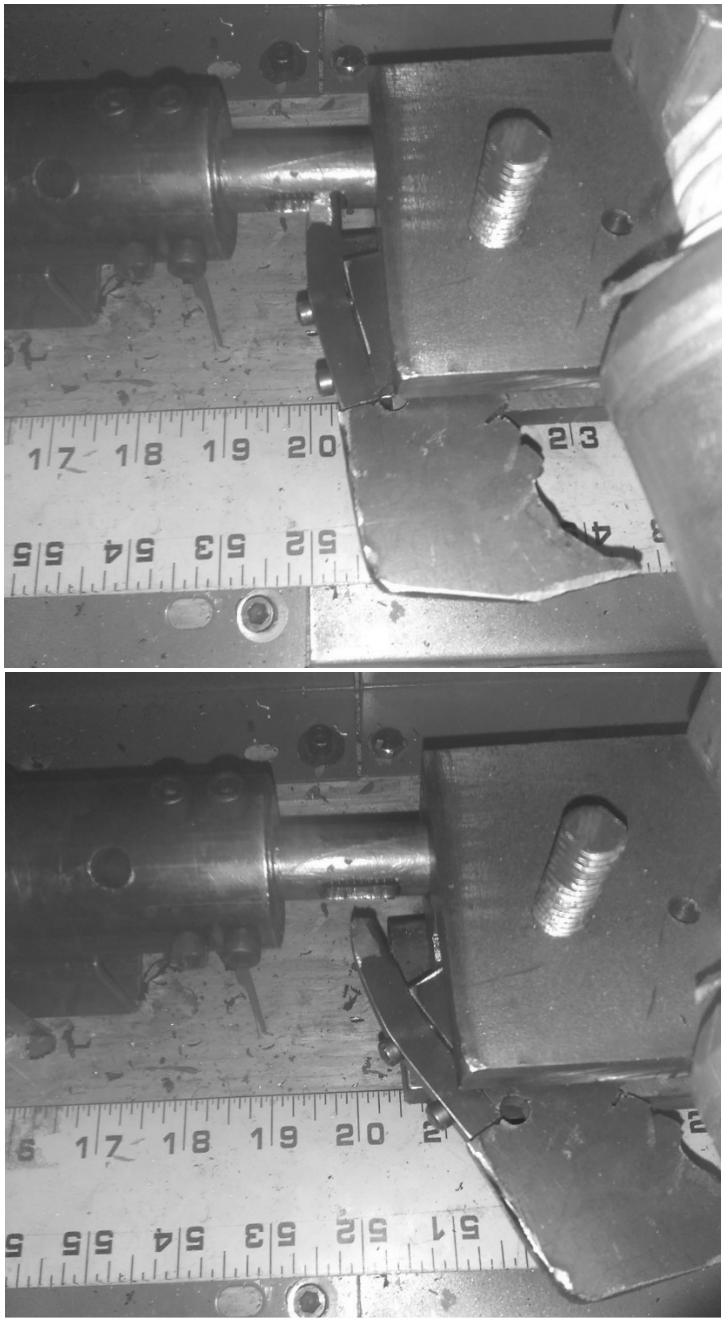

Fig. 12: Detail of release lever showing open and closed positions.

The release lever was cut from 1/4″ thick mild steel plate with a hacksaw and filed to its final dimensions. The section of the release lever that engaged with the piston shaft was identified as a potential wear surface and was made a separate component which was screwed to the release lever with a pair of 8-32 screws. As can be seen in Fig. 12,

the release lever pivoted to the open position. The release lever sear occupied the space that the release lever pivoted into. The gun was fired by actuating a geared servomotor, which rotated the sear out of the way of the release lever and allowed it to pivot.

3.1.4 Gas Supply, Barrel and Driving Section Cylinder

Regulated nitrogen was supplied to the gun by a ¼″ stainless steel line. At the gun, the line was split by a T-junction into driving section and driven section lines. For the purpose of leak checking, each line was provided with a shutoff valve. A drain valve was placed on the driven section line to vent the system in the event of a misfire.

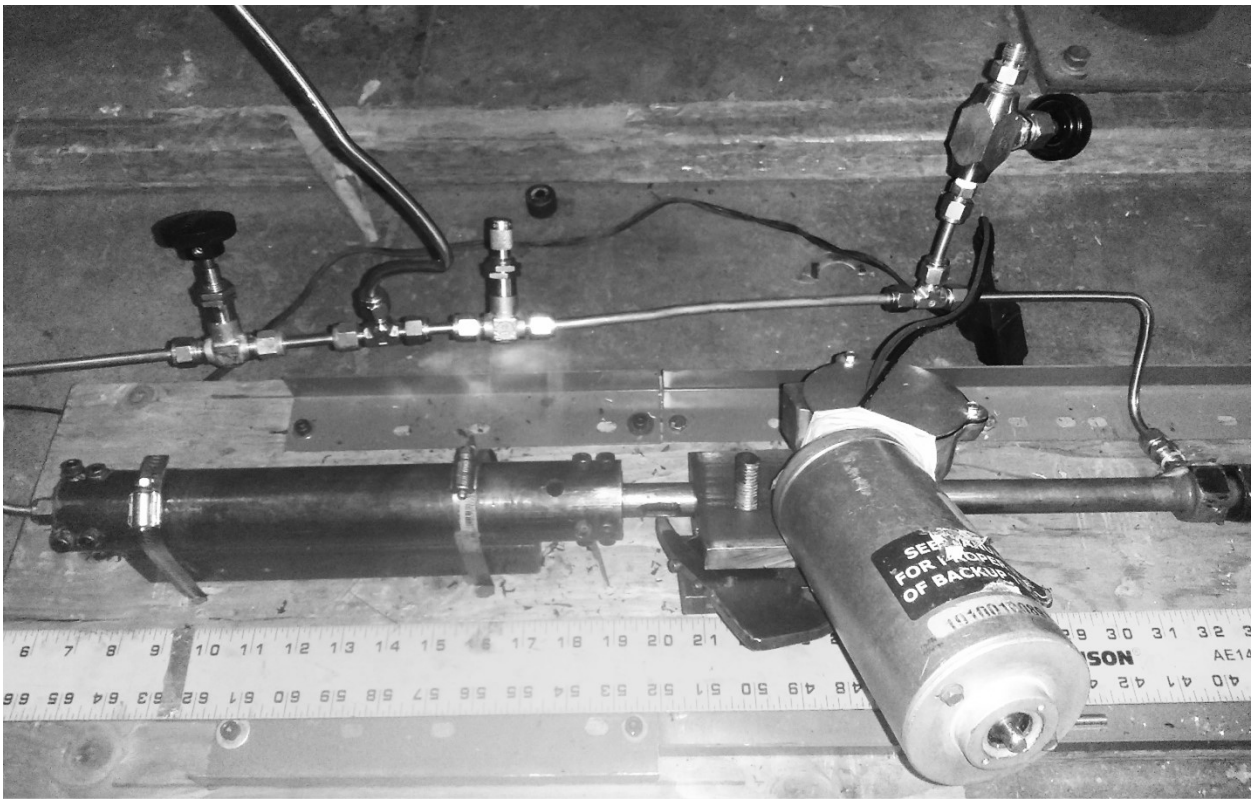

Fig. 13: Gas supply detail. Left to right: driving section shutoff, driven section shutoff, drain valve.

The driving section cylinder was constructed from a 12″ length of 1 ¼″ ID x 1 ¾″ OD seamless pipe. The interior of the pipe was wet honed to improve piston sealing. Adaptor blocks for the barrel tube and the ¼″ NPT gas supply fitting were fixed to each end by eight ¼″ bolts. The holes were drilled on a laboratory drill press using a jig for

accurate location and tapped to ¼”-20. The adaptor block for the gas supply fitting was sealed with JB-Weld.

3.2 Experimental Procedure

Prior to each firing, the piston was reset to its initial position by advancing a rod from the muzzle of the gun towards the driving section. The projectile was weighed, fitted with a ½” OD o-ring and coated in vacuum grease before being thrust down the muzzle until it encountered the shear pin fitting. The projectile was rotated until its shear pin hole aligned with the threaded holes in the shear pin fitting. The shear pin was advanced through the fitting and the projectile. The piston retaining lever was reset and the retaining lever sear was rotated to support it. The servomotor which controlled the position of the sear was tested. Test recordings were taken with the Phantom v1211 high-speed camera. The lab was evacuated whenever a shot was about to take place.

The valves to the driving and driven section were opened and the drain valve was closed. The gas supply to the gun was opened and the regulator was brought to the desired fill pressure. For the three shots described in Chapter 4, this pressure was always 1400 psi. The servomotor was activated, the sear rotated away from the retaining lever, and the gun fired. The gas supply was closed, the projectile was recovered, and the velocimetry video was trimmed to the projectile transit period.

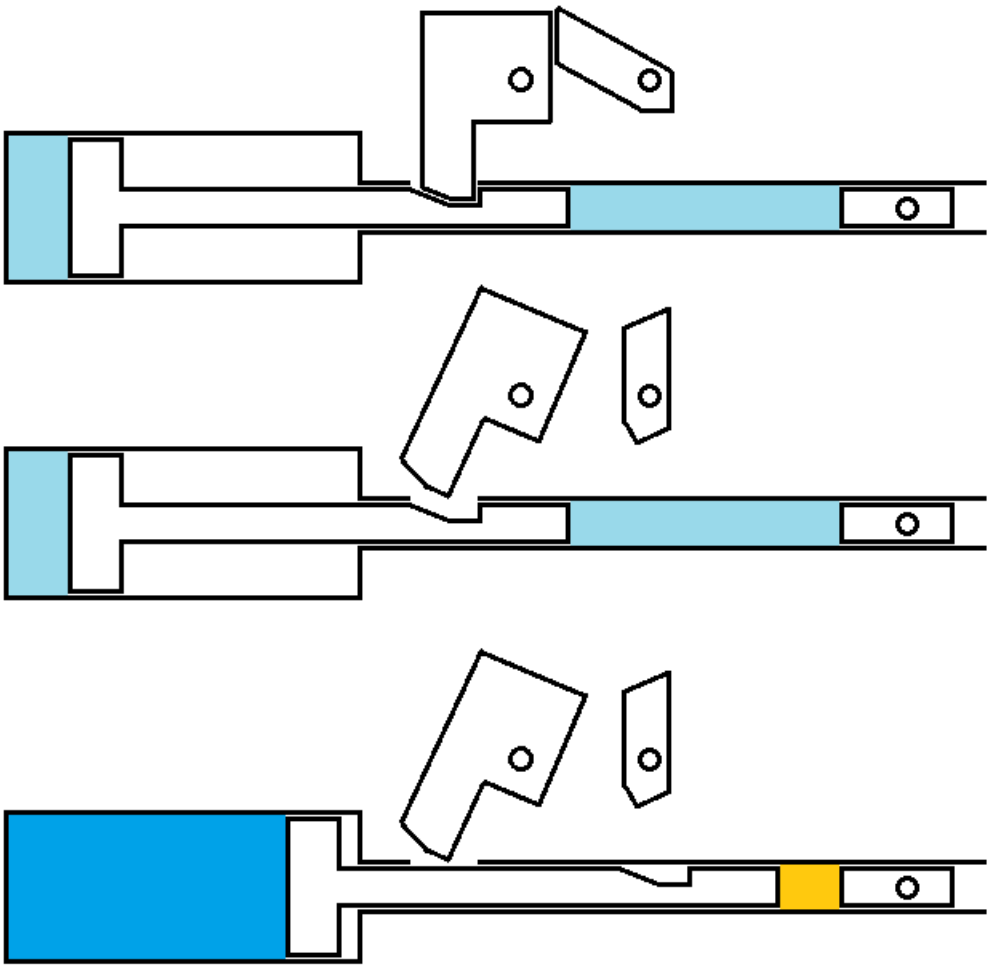

Fig. 14: TSGG operation.

The small scale and improvised nature of this TSGG resulted in rapid pressure drops in the driven section if the driven section isolator valve was shut. To ensure repeatable results, it was necessary to leave the isolator valve open during firing so that leaking gas could be replaced up to the moment of firing. It was found during testing that the driving section seal was excellent, and only an abundance of caution with regards to the repeatability of results prevented investigation into the use of different fill pressures in the driving section and driven section.

3.3 Velocimetry

The muzzle of the gun was placed in the focus of a Phantom v1211 high-speed camera recording at 50,000 frames per second. The wealth of data collected by a high-speed camera was desirable, as was the expediency of using equipment already present in the lab instead of improvising some other method of velocimetry.

Fig. 15: Velocimetry collection area.

The camera recorded an area between the muzzle and the catcher tube which was backed by a piece of athletic tape with marks at half-centimeter intervals. As it left the muzzle, the projectile traveled in front of these marks. The distance traveled by the projectile in each frame could be directly measured and the velocity of the projectile could be found by multiplying the distance in meters by the framerate.

The apparent velocity of the projectile could appear to oscillate from frame to frame due to sources of noise in the projectile location. These included water vapor clouds created

by shocks on the projectile nose, errant droplet clouds of silicone vapor, and pieces of the projectile. To reduce the influence of noise, the projectile velocity was measured from the time taken to transit the entire measurement tape. The influence of aerodynamic drag on the projectile velocity over that distance is calculated in Chapter 4 and found to be minimal.

Chapter 4

RESULTS

After a six-shot break-in period, a series of three shots were fired with the goal of demonstrating increased performance derived from temperature multiplication in the driven section. Each shot was performed with the same initial conditions in the driven section and driving section. The projectile mass was decreased with each shot to demonstrate a trend of increasing velocity and decreasing ballistic efficiency with decreasing projectile mass. Shot #7 used a projectile with a mass of 5.8 g, shot #8 was at 3.8 g and shot #9 was 3.25 g. The gun was prefilled with nitrogen gas at a pressure of 1400 psi and at room temperature for all three shots.

The aluminum shear pin was calculated to provide a breaking pressure of 10500 psi or 72 MPa after accounting for strain rate effects:

$$P = \frac{(30{,}000\ psi - 1450\ psi) * 2 * (0.036\ in^2)}{\pi * (0.25\ in)^2} = 10500\ psi \tag{4.1}$$

Where 0.036 in^2 is the tensile cross-sectional area of a ¼″-28 threaded rod. This area is multiplied by two due to the assumption that the pressure load is shared equally by each face of the pin that exits the sides of the projectile.

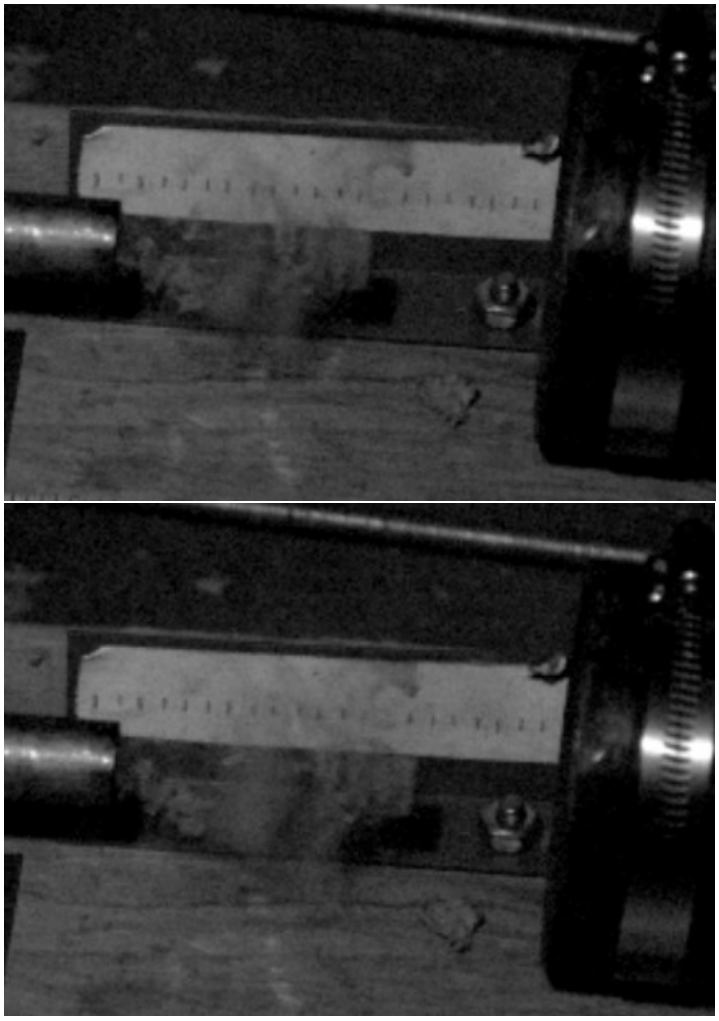

Fig. 16: Shot #9 velocimetry data.

The position of the projectile was measured on a frame-by-frame basis and also over the entire transit of the measurement area. A cylinder travelling in air at room temperature and pressure at 450 m/s has a drag coefficient of approximately 1.25, and the air has a density of 1.2 kg/m^3, so the drag force exerted on the 12.7 mm diameter projectile is:

$$F = \frac{(1.25)(1.2\ kg/m^3)\left(450\frac{m}{s}\right)^2(0.000127\ m^2)}{2} = 20\ N \tag{4.2}$$

This translates to a deceleration of 6150 m/s^2 for a 3.25 gram projectile. The projectile transited the measurement area in about 250 µs, losing about 1.5 m/s of velocity. For

the purposes of velocimetry, then, the projectile was assumed to have a constant velocity over the measurement area.

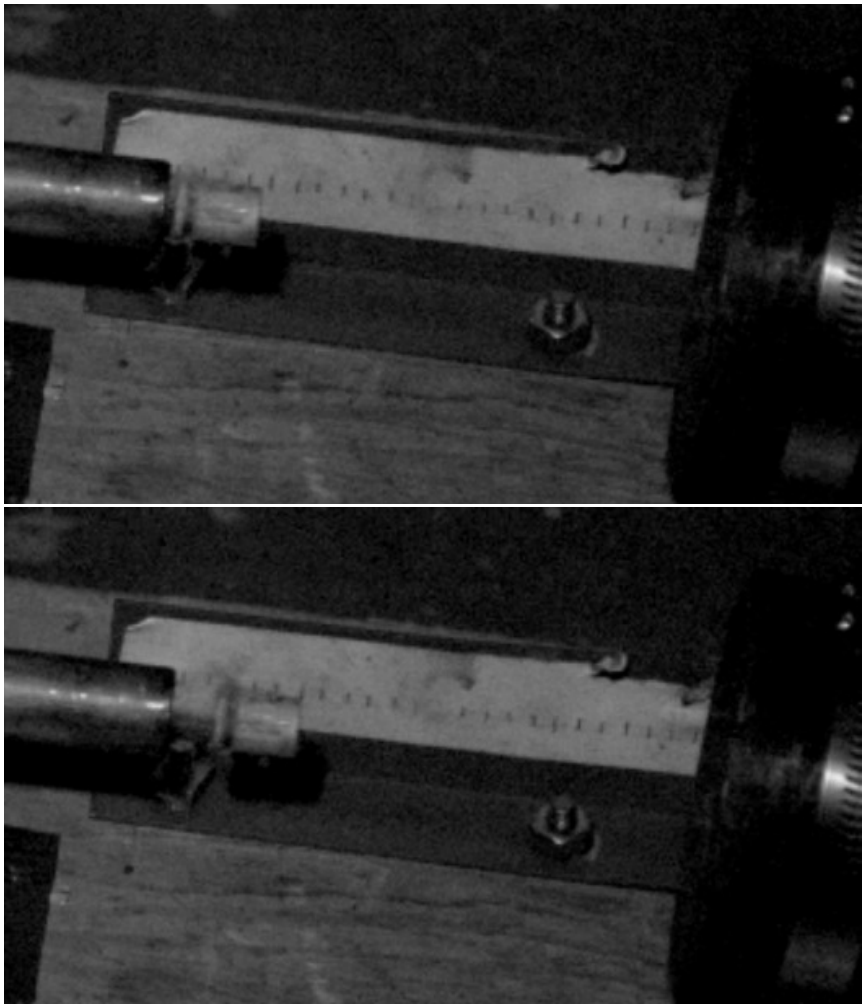

Fig. 17: Shot #7 velocimetry data.

4.2 Muzzle Pressure Inference

The high-speed video of the projectile exiting the nozzle provided an interesting opportunity to find the residual gas pressure at the nozzle with an existing empirical correlation. The muzzle of a gun produces a barrel shock as propellant leaves the muzzle behind the projectile. A barrel shock is a structure characteristic of underexpanded supersonic flow which is defined by the interaction of expansion waves

emanating from the lip of the muzzle and compression waves traveling towards the centerline of the jet [7].

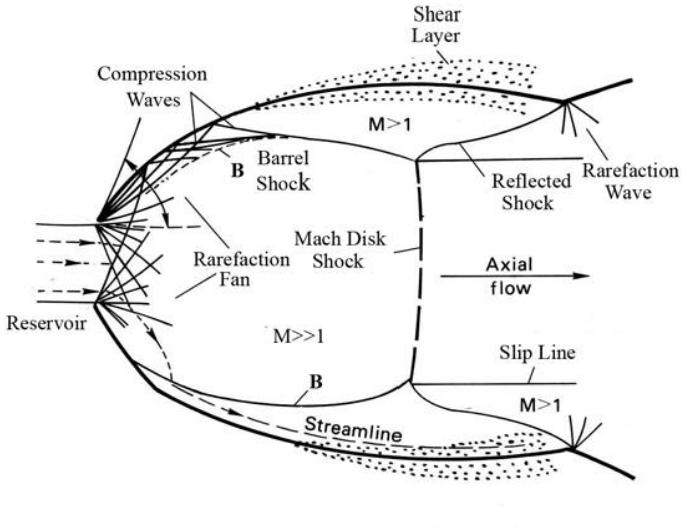

Fig. 18: Underexpanded jet structure. From [7].

The length between a nozzle exit plane and the Mach disk of the jet issuing from the nozzle increases with the stagnation pressure of the gas traveling through the nozzle. A review of jet studies [8] found that measurements of barrel shock length collapsed on a single curve over a variety of conditions.

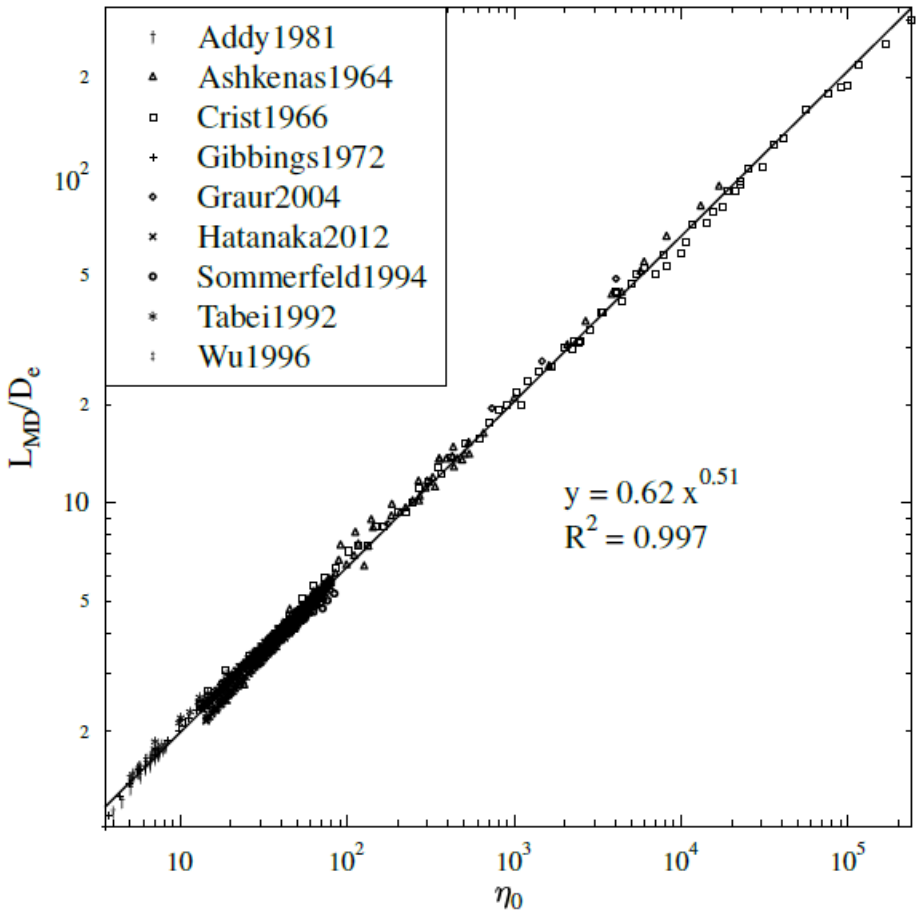

Fig. 19: Variation of Mach disk length/nozzle diameter ratio with ambient pressure/stagnation pressure ratio. From [8].

The jet issuing from the muzzle of the gun is visible in the velocimetry images as a vapor cloud behind the projectile. Because the Mach disk length is so dependent on the pressure ratio between the jet and the surroundings, it was necessary to advance the recording to a point where the initial shock bubble from the muzzle has cleared away and steady flow was established.

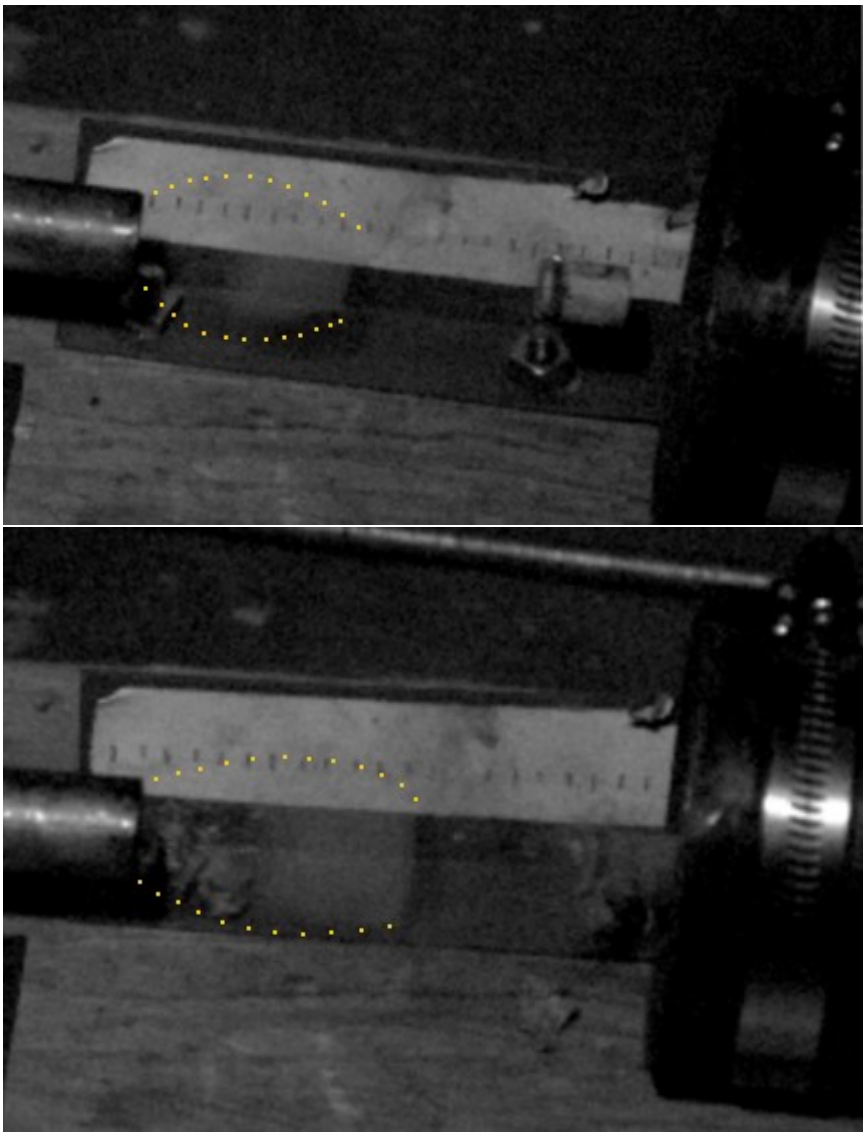

Fig. 20: Barrel shock dimensions for shot #7 (top) and shot#9 (bottom).

For both shot #7 and shot #9, the Mach disk length/muzzle diameter ratio was 3.5, corresponding to a residual pressure of 430 psi at the muzzle.

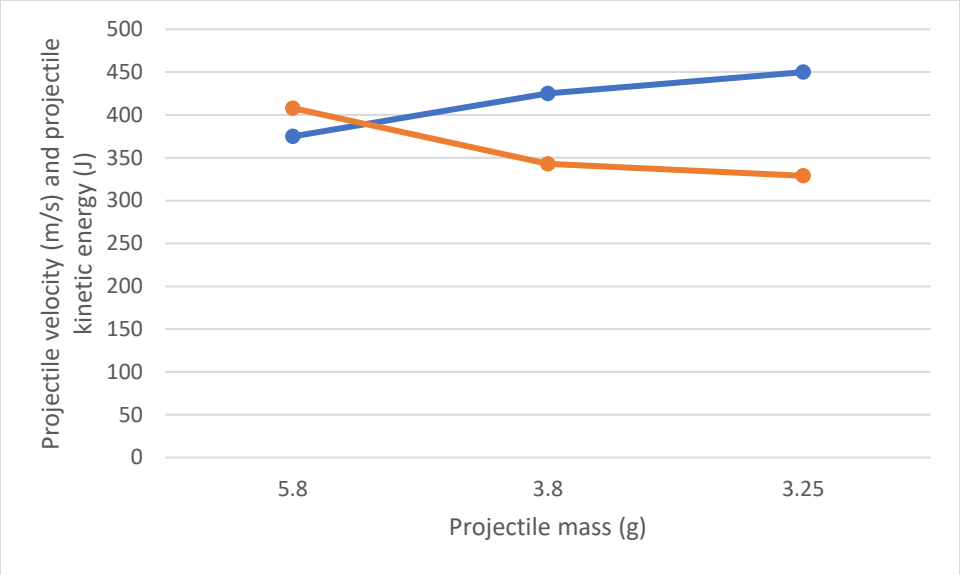

Fig. 21: Variation of projectile energy and velocity with projectile mass.

As projectile mass decreased, projectile velocity increased. Mach effects made themselves known through the decrease in projectile energy. This is a good example of well-known inverse relationship between the efficiency of acceleration and the fraction of the propellant sound speed at which the projectile is traveling. This relationship (Eqn. 4.3) was set forth for the case of infinite-breech guns by Seigel (Eqn. 11-6 in [5]) and also Higgins [9].

$$\frac{p_p}{p_0} = \left[1 - \frac{(\gamma - 1)}{2}\frac{u_p}{a_0}\right]^{\frac{2\gamma}{\gamma - 1}} \tag{4.3}$$

The ratio of the projectile base pressure P_p to the chamber pressure of the gun P_0 is a function of the projectile velocity u_p to the initial propellant sound speed a_0.

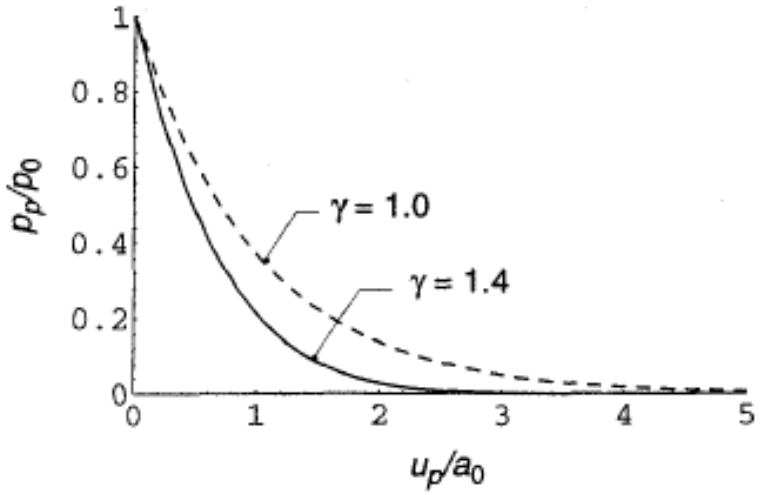

Fig. 22: Projectile base pressure as a function of projectile velocity. From [9].

The ballistic efficiency is defined here as the kinetic energy of the projectile divided by the 0-D isentropic expansion energy available to the propellant in the driven section. This 0-D isentropic expansion energy is the energy which would be imparted to the projectile if no Mach effects were present. The wall-plug efficiency of the gun is defined here as the kinetic energy of the projectile divided by the amount of energy required to isothermally compress the nitrogen in both the driving and driven sections to 1400 psi. The volume of the driven section at the time of firing is, according to the piston motion code, about 4.6 mL. The volume of the barrel is 57 mL. The temperature of the propellant at the time of firing is 520 K and there is 2.3 g of propellant in the driven section.

$$U = -(520\ K)\left(1000\frac{J}{kgK}\right)(0.0023\ kg)\left(\left(\frac{4.6mL}{57mL}\right)^{\gamma-1} - 1\right) = 760\ J \tag{4.4}$$

So, the ballistic efficiency of shot #9 was approximately 43%. The driven section contained 2.3 g of nitrogen and the driving section contained 7.1 g of nitrogen. The isothermal compression energy is:

$$U = (293\ K)\left(1000\frac{J}{kgK}\right)(0.0094\ g)Ln\left(\frac{1400\ psi}{14.7\ psi}\right) = 12{,}550\ J \tag{4.5}$$

So, the wall-plug efficiency of shot #9 is 2.6%. The high ballistic efficiency of the shot is good evidence that high temperatures were achieved in the driven section.

Chapter 5

CONCLUSION

A subscale TSGG operating off of 1400 psi nitrogen was designed and constructed to test the performance enhancing effect of rapid compression. The velocities achieved during testing showed the validity of the basic temperature/pressure multiplying concept. A 3.25 g projectile was accelerated to 450 m/s at a barrel length of 36 calibers (18”). An infinite-breech gun using room-temperature nitrogen at 1400 psi as a propellant would have achieved velocities 20%-25% lower than were achieved with this gun. Several technical paths to increased performance were found during the course of testing.

5.1 Future work

During testing, a number of areas for improvement in the TSGG were identified. Some of these were engineering issues specific to the gun itself and others were conceptual. First, the high piston speed was the cause of excessive wear on the driving section seals. Even the hardest bronze-filled PTFE sealing rings are rated for approximately 15 m/s, and the piston achieved a maximum of 50 m/s. In order to get an acceptable seal on the piston prior to firing while minimizing seal wear during firing, face seals should be used on the piston and the piston shaft should rest on bronze or cast-iron wear surfaces, as in an ICE piston.

Second, designing the gun to use gas at relatively high pressure (1400 psi) limited the achievable compression ratio and therefore the achievable temperature in the driven section. Higher projectile velocities could be achieved by reducing the prefill pressure to approximately 300 psi and increasing the size of the gas reservoirs to compensate for the reduced density of the gas.

Third, making the driven section an extension of the barrel with the same ID necessarily made the driven section relatively long in order to contain sufficient gas to drive the

projectile. This resulted in a relatively long, skinny piston (Fig. 9) which was vulnerable to buckling failure. It would probably not be possible to reduce the fill pressure if the driven section remained at the same ID as the barrel because the driven section would become extremely long. The piston shaft would then be almost guaranteed to buckle.

Fourth, the retaining lever experienced significant wear with each shot despite efforts to minimize wear. Scaling up the TSGG would only exacerbate this issue. It would be preferable to use some sort of non-mechanical means of holding the piston in place, or to use some sort of release pin which is destroyed with each firing in the same way that a burst diaphragm is.

BIBLIOGRAPHY

[1] Hertzberg, A., Bruckner, A. P., and Bogdanoff, D. W., "**Ram Accelerator: A New Chemical Method for Accelerating Projectiles to Ultrahigh Velocities**," *Journal of Propulsion and Power*, Vol. 14, No. 6, Nov. - Dec., 1988, pp. 195-203.

[2] Byrd, T., "**Experimentally-Driven Model for the Baffled Tube Ram Accelerator**," Master's thesis, University of Washington, 2018.

[3] Leege, B. Personal communications, March, 2021.

[4] Bogdanoff, D.W. "**Preliminary Assessment of the Use of Heavy Gases in Two-Stage Light Gas Guns**," *69th Meeting of the Aeroballistic Range Association*, Bath, England, October 7-October 12, 2018.

[5] Seigel, A.E. "**The Theory of High-Speed Guns**," *AGARDorgraph 91*, May, 1965.

[6] Manes, A., Peroni, L., Scapin, M., and Giglio, M. "**Analysis of Strain Rate Behavior of an Al 6061 T6 Alloy**," *Engineering Procedia,* Vol. 10, 2011, pp. 3477-3482.

[7] Orescanin, M. M., Priscoy, D., and Austinz, J. M., "**Exhaust of Underexpanded Jets from Finite Reservoirs**," AIAA 2010-5108, July 2010.

[8] Franquet, E., Perrier, V., Gibout, S., and Bruel, P. "**Free Underexpanded Jets in a Quiescent Medium: A Review**," *Progress in Aerospace Sciences*, Vol. 77, 2015, pp. 25-58.

[9] Higgins, A. J., "**A Review of Distributed Injection Hypervelocity Accelerators**," *Joint Propulsion Conference and Exhibit*, Seattle, 1997

Appendix A

PISTON MATLAB CODE

```
clc;
close all;
clearvars;

%Firing conditions
P_break=72*10^6;   %Firing pressure (Pa)

%Intrinsic properties and ICs
R=287;          %Specific gas constant
T0=293;         %Initial temperature (K)
P0=2.07*10^6;      %Initial pressure (Pa)
k=1.4;          %Ratio of specific heats
Cp=1000;        %Specific heat capacity (J/kgK)

%Piston and cylinder dimensions
V0_drvr=400;    %Initial driver section volume (m^3)
V0_drvn=120;  %Initial driven section volume (m^3)
A_drvr=28;   %Driver piston area (m^2)
A_drvn=1.77;   %Driven piston area (m^2)
m_piston=40000;    %Piston mass (kg)

%Calculated properties
m_drvn=V0_drvn*P0/(R*T0);   %Gas mass in driven section
m_drvr=V0_drvr*P0/(R*T0);   %Gas mass in driving section
L_drvn=V0_drvn/A_drvn;      %Initial length of driven section

%Calculation matrices
dt=0.0001;      %Time step size
tf=0.5;         %Final time
t=0:dt:(tf-dt); %Time step storage matrix
T_drvn=zeros(1,length(t));   T_drvn(1)=T0;  %Driven section temperature
T_drvr=T_drvn;           T_drvr(1)=T0;      %Driving section temperature
P_drvn=T_drvn;           P_drvn(1)=P0;      %Driven section pressure
P_drvr=T_drvn;           P_drvr(1)=P0;      %Driving section pressure
V_drvn=T_drvn;           V_drvn(1)=V0_drvn; %Driven section volume
V_drvr=T_drvn;           V_drvr(1)=V0_drvr; %Driving section volume
x=zeros(1,length(t));   %Piston position
vel=x;                  %Piston velocity
acc=x;                  %Piston acceleration

%Calculation loop
for i=1:length(t)-1
   if x(i) > L_drvn || P_drvn(i) > P_break
       Tf_drvr=T_drvr(i);
       v_final=vel(i);
       Tf_drvn=T_drvn(i);
       break
   end
   %Piston kinematics
   acc(i+1)=(A_drvr*P_drvr(i)-A_drvn*P_drvn(i))/m_piston;
   vel(i+1)=vel(i)+dt*acc(i);
   x(i+1)=x(i)+vel(i)*dt;
   %Driver and driven section gas properties
```

```
    V_drvr(i+1)=V0_drvr+x(i)*A_drvr;
    V_drvn(i+1)=V0_drvn-x(i)*A_drvn;
    P_drvr(i+1)=P0*(V0_drvr/V_drvr(i+1))^k;
    P_drvn(i+1)=P0*(V0_drvn/V_drvn(i+1))^k;
    T_drvr(i+1)=T0*(V0_drvr/V_drvr(i+1))^(k-1);
    T_drvn(i+1)=T0*(V0_drvn/V_drvn(i+1))^(k-1);
end

figure('Name','Temperature');
plot(t(1:i),T_drvn(1:i),t(1:i),T_drvr(1:i));
figure('Name','Pressure');
plot(t(1:i),P_drvn(1:i),t(1:i),P_drvr(1:i));
figure('Name','Piston velocity');
plot(x(1:i),vel(1:i));
figure('Name','Volume');
plot(t(1:i),V_drvr(1:i),t(1:i),V_drvn(1:i));

%Energy balance sanity check
(m_drvn*(Tf_drvn-T0)*Cp+0.5*m_piston*v_final^2)/(m_drvr*(T0-Tf_drvr)*Cp)
```

Appendix B

PROJECTILE MATLAB CODE

```
clc;
close all;
clearvars;

m=0.00325;
D=0.0127;
P0=10*10^6;
a0=350;
dt=0.00001;
k=1.4;
tf=0.002;

t=(0:dt:tf);
x=zeros(size(t));
P=x;
vel=x;
acc=x;

for i=1:length(x)-1
    P(i)=P0*(1-0.1*vel(i)/a0)^12;
    acc(i+1)=P(i)*pi*0.25*D^2/m;
    vel(i+1)=vel(i)+dt*acc(i);
    x(i+1)=x(i)+vel(i)*dt;
end
figure('Name','Velocity');

plot(x,vel);
xlabel('Barrel length (m)');
ylabel('Velocity (m/s)');
```